

IMPROVEMENTS TO RADIATION ON UPPER-LEVEL WRF PERFORMANCE OVER THE ANTARCTIC

Jordan G. Powers, Steven M. Cavallo, and Kevin W. Manning
Mesoscale and Microscale Meteorology Division
NCAR Earth System Laboratory, National Center for Atmospheric Research
Boulder, Colorado, USA

1. INTRODUCTION

Analyses of WRF simulations over the Atlantic have revealed problems in WRF's behavior near the model top. The current study looks at WRF's upper-level performance over Antarctica in the context of the Antarctic Mesoscale Prediction System (AMPS) (Powers et al. 2003). AMPS is a real-time, experimental, NWP system providing numerical guidance to forecasters of the United States Antarctic Program (USAP). In addition, it provides support for American and international research, field campaigns, and logistical needs over Antarctica. AMPS employs the Weather Research and Forecasting (WRF) model (Skamarock et al. 2008).

An ongoing aspect of the AMPS effort is the tuning of WRF physics to improve forecast performance over Antarctica/polar regions. This work examines WRF's radiative response at upper levels over Antarctica and the relation to the longwave (LW) radiation scheme. Modifications to the LW package are tested in summer and winter season AMPS forecast experiments. These are analyzed to determine the impacts and whether to implement the modified scheme operationally. For the first time, the issues of WRF radiative flux errors and heating issues at high levels over the polar latitudes are addressed.

2. BACKGROUND AND MODEL CONFIGURATION

a. Motivation

Analyses of WRF simulations during the 2009 hurricane season in the Atlantic Basin brought to light the potential for radiation-induced problems near the model top. The results from simulated periods showed a distinct cooling at upper levels, and Cavallo et al. (2010) present the background on this work. As an example, Fig. 1(a) shows the evolution of potential temperature (θ) over time (mean removed) averaged over the Atlantic Basin domain from the 2009 season examination. Near the model top temperatures begin relatively warm and become progressively cooler. Here, WRF was run in cycling mode with data assimilation performed through an ensemble Kalman filter approach. Figure 1(b) presents the differences of WRF and the GFS (Global Forecasting System) analyses through the test period. Compared to the

analyses, WRF displays a cool bias aloft, and this reaches close to -10K during this period (although the scale in Fig. 1 only reaches -4K). Cooling tendencies at the WRF model top in similar analyses by these investigations have also been found to be up to -10K/day.

The cool bias is a result of the approaches used in the longwave radiation scheme employed, the RRTM (Rapid Radiative Transfer Model) (Mlawer et al. 1997). Specifically, this scheme makes assumptions about the conditions above the model top to the top of the atmosphere (TOA) for the calculation of the radiative fluxes at the model upper boundary. The formulation leads to much of the error seen.

In making its flux calculations, the scheme internally uses one additional level between the model top and the TOA. In the new layer the temperature is assumed isothermal and the mixing ratios, except for that for O_3 , are assumed constant. These assumptions can be inaccurate, however, for T and q_v for WRF with relatively low model tops (compared to the tops in global models for which the scheme was originally targeted). Actual temperatures in computational layers above 50–10 hPa (a region more commonly used for the top levels in most WRF applications) can vary significantly from those based on an assumed temperature equal to that of the model top. In addition, inaccurate assumptions in stratospheric relative humidity can produce conditions that are far too moist. That excessive moisture is then carried to the TOA through the buffer layer by the assumption.

Thus, modifications have been developed to improve the RRTM scheme's treatment of buffer layer conditions and its calculations of longwave fluxes. The following changes to the scheme have been made and are tested in the experiments described below.

– Extra levels are added above the model top. Several levels are added in the RRTM layer from the model top to the TOA to serve as a buffer. The layer spacing is $\Delta p = 2.5$ hPa. Note that these levels only occur within the RRTM longwave package for its calculations and do not add to the number of WRF η -levels. Thus, the additional computation is not large, and the overall run time is not increased significantly.

– Temperatures in the new levels are interpolated from an average observed temperature curve reflecting conditions in the stratosphere.

– The water vapor mixing ratio is set to a value of 1×10^{-6} kg/kg in buffer layers.

Figure 2(a) shows the additional levels and temperatures for calculation in the scheme. In this example, the new levels are at 2.5 hPa increments from the model top to the TOA. For the AMPS testing configuration (described below), this is from 10 hPa to the TOA. The temperatures at the additional levels are derived from a temperature profile composited from the observed profiles of different regions. Figure 2(b) shows the profiles for various regions (tropical, mid-latitude winter, mid-latitude summer, and sub-Arctic winter) (Ellingson et al. 1991) and the resultant average curve. The average is used for this version of the modifications to make the revised scheme applicable globally, instead of trying to produce regionally-tuned versions. The temperatures applied at the extra levels are based on the average profile and the difference from the average profile seen at the model top. The differences in the temperature at the various buffer levels can be seen in Fig. 2(a), which shows the temperature curve applied (solid) with the one that would have been used following an isothermal assumption (dashed).

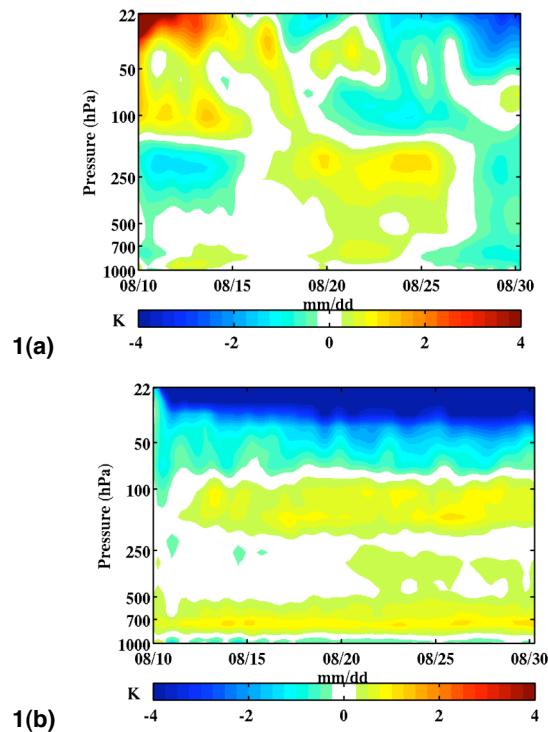


Fig. 1: (a) WRF domain-averaged hr-6 θ perturbation (K; temporal mean removed at each level) from surface to model top for 10–30 August 2009 over the Atlantic Basin hurricane domain. (b) Domain-averaged WRF–GFS analysis θ (K) for 10–30 August 2009 over Atlantic Basin domain.

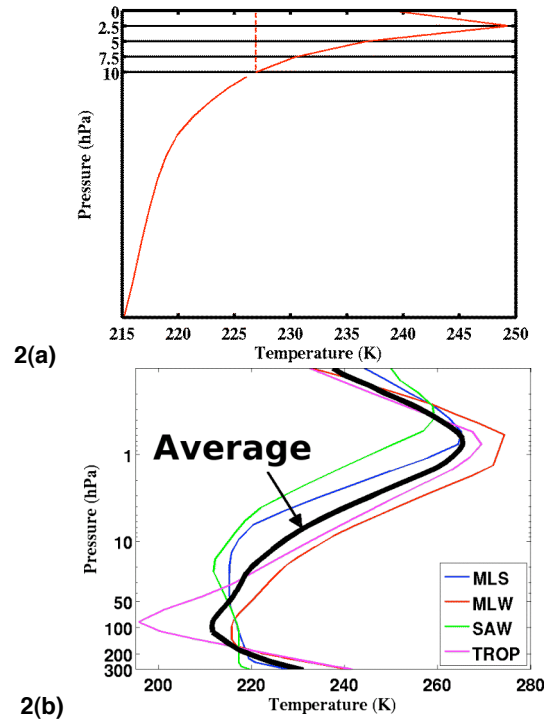


Fig. 2: Extra levels in modified RRTM longwave scheme and average temperature profile used. (a) Schematic of extra computational levels used in RRTM longwave scheme. Vertical spacing of levels is 2.5 hpa. Solid curve= Temperatures used at extra levels. Dashed curve= Temperatures reflecting original isothermal layer temperature assumption. (b) Regional observed temperature profiles and averaged profile used in modified scheme. MLS= mid-latitude summer; MLW= mid-latitude winter; TROP= tropical; SAW= sub-Arctic winter.

b. Model Configuration

WRF is tested in AMPS for summer and winter periods to diagnose the potential upper-level cooling and temperature biases. Shown in Fig. 3, the grid configuration features the two coarsest AMPS grids, with 45-km and 15-km horizontal spacings. The test periods are January 1–7, 2010 (austral summer) and July 1–7, 2009 (austral winter). Model heating/cooling rates for longwave and shortwave processes are compared against observed profiles for different global regions.

AMPS Testing Setup

2 domains: 45 km, 15 km
 Vertical levels: 44 levels
 Model top: 10 mb
 IC/BC: GFS analysis/GFS forecast BCs
 Simulation lengths: 6 hrs
 Periods: January 2010 (summer), July 2009 (winter)
 Radiation: RRTM longwave, Goddard shortwave

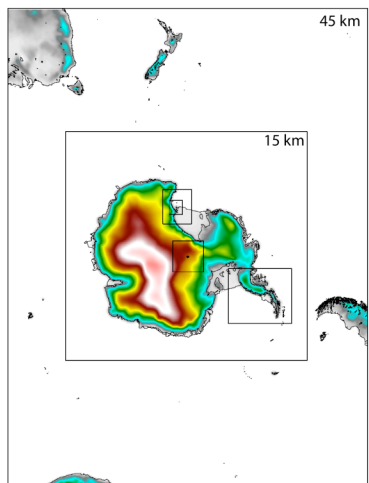


Fig. 3: AMPS WRF domains used for experiments. Outer grid: 45-km spacing. Inner grid: 15-km spacing. Grid outlines shown within 15-km grid are not run for the experiments.

3. RESULTS

WRF is first run with the AMPS grids with the unmodified RRTM scheme to assess model behavior near the model top. Figures 4(a) and 4(b) show the heating rate biases in the winter and summer test periods. The heating rates are composited over the 15-km inner domain. Here, the comparison is between model heating profiles derived from averaged WRF 6-hr forecasts and heating profiles (not shown) for the sub-Arctic regions for winter and summer. The sub-Arctic profiles are used as the closest available that may be comparable to the southern high-latitude areas modeled.

The winter results show a net positive daily heating bias overall, with this being primarily due to the longwave component. Here this most likely reflects that the conditions in the southern polar vortex would be colder than those reflected in sub-Arctic winter heating/cooling profiles. As radiative emission (and cooling) is proportional to temperature, the longwave cooling over the colder (aloft) region covered by the AMPS grids would be less.

The summer results show a cooling bias above 100 hPa. The longwave contribution is maximized at the model top. The shortwave bias increases, too, above 100 hPa, but decreases at the model top level. Overall, WRF has net cooling aloft, as had been seen in the Atlantic Basin tests. In summary, WRF shows an upper-level/model top cooling bias in the Antarctic in the warm season, although the errors are not as large as in the mid-latitudes.

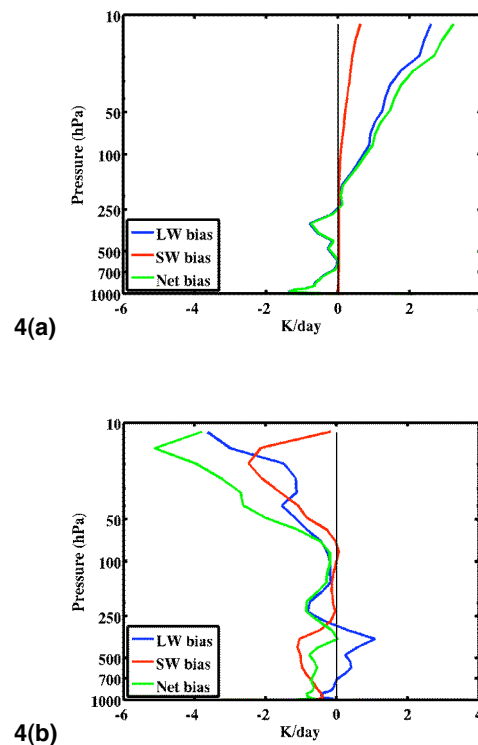


Fig. 4: AMPS WRF heating rate biases. Profiles of differences in heating rates from longwave (LW), shortwave (SW), and net (LW + SW) processes. (a) AMPS-SAW (Sub-Arctic Winter). (b) AMPS-SAS (Sub-Arctic Summer).

The experiment consists of runs the modified RRTM scheme in AMPS for the given seasons. Figure 5 compares heating rates for the control run (original RRTM) with the experiment (modified RRTM), along with standard profiles for mid-latitude and sub-Arctic regions. For the winter period (Fig. 5(a)) the control and experiment are largely similar: both have a bias toward warming (less cooling) (compared to the observations) at the model top. While both do have lower cooling rates than the given observations, it is noted that the standard profiles compared against are for the mid-latitudes and sub-Arctic, not for Antarctica.

For summer, both the control and the experiment show biased cooling above 75 hPa compared to the observations. However, the experiment shows

decreased biases right at the model top. The model top bias reduction is 2 K/d.

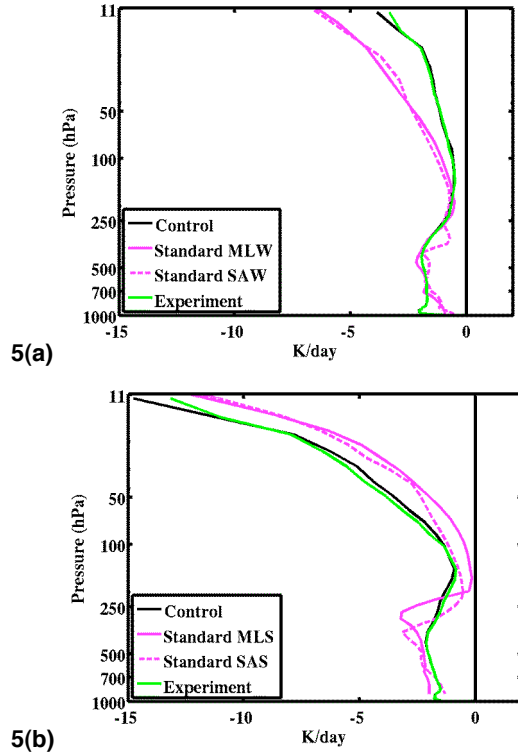


Fig. 5: Observed v. AMPS test heating rates. Control= Original RRTM scheme. Experiment= Modified RRTM scheme. (a) Winter (July 2009). MLW= Mid-Latitude Winter; SAW= Sub-Arctic Winter. (b) Summer (January 2010). MLS= Mid-Latitude Summer; SAS= Sub-Arctic Summer.

Figure 6 isolates the experiment differences. For the winter period (Fig. 6(a)) only slight differences are seen, except for the top model level, where the difference in rates is positive (+.5 K/d) (modified scheme cooling less than original). For summer (Fig. 6(b)), the experiment shows more cooling than the control below the model top (.5 K/d), but significantly less at the model top 2 K/d¹.

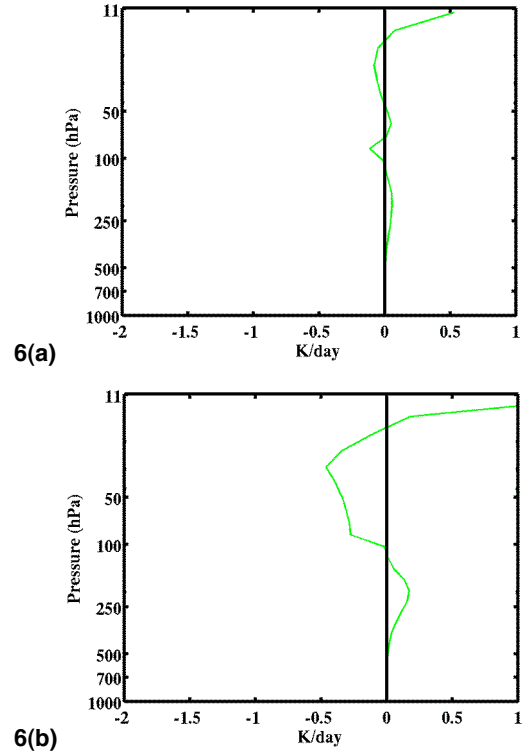


Fig. 6: Heating rate differences (K/day): Experiment–Control. (a) Winter (July 2009). (b) Summer (January 2010).

Figures 7 and 8 show the heating/cooling rates at the model top (top $\frac{1}{2}$ - η level) for the experiments. In winter, $\partial\theta/\partial t$ from LW processes is negative in both runs, with the control showing greater cooling (Figs. 7(a), (b)). In these plots (including 7(a),(b),(c); 8(a),(b),(c)) the heating rates for LW processes are calculated as instantaneous rates averaged at hour 6 of the forecasts for the test periods. The change from the modified scheme averages about .5 K/d over the domain (Fig. 7(c)). The overall potential temperature change rate difference, $\partial\theta/\partial t_{\text{total}}$, averages .1-.2 k/d (Fig. 7(d)). Here, these $\partial\theta/\partial t_{\text{total}}$ values reflect the rates of change as calculated over hrs 0–6 of the forecasts in the test periods.

The summer differences are more substantial (Figs. 8(a),(b)). Over the continent, the original scheme rates are approximately -15.5 K/d, while the modified scheme rates are approximately -13.5 K/d. The LW cooling rates are 1.5–2 K/d less with the modified scheme (Fig. 8(c)). And, the overall potential temperature cooling rates at the model top are decreased up to .5 K/d over the continent (Fig. 8(d)). This can translate to differences in model top temperatures of about 2.5 K during the 5-day AMPS forecasts. Note, too, that the erroneous LW cooling rates seen as points in Fig. 8(a) and in the difference

¹ Note that scale in plot is capped at 1 K/d. Actual differences values reach 2 K/d at the model top level.

plot in 8(c), which reflect biases in radiosonde RH observations, are also corrected by the modifications.

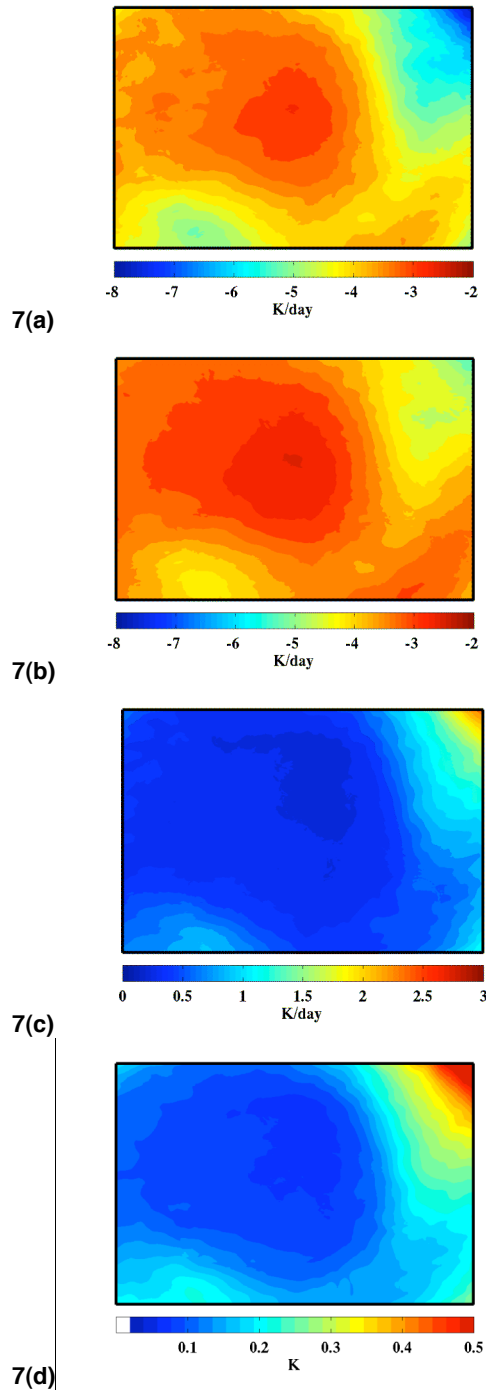


Fig. 7: Heating rates from LW and total in AMPS WRF tests for winter (July 2010) period. $\partial\theta/\partial t$ LW rates ((a), (b), (c)) based on instantaneous values for forecasts at hr 6. Total $\partial\theta/\partial t$ rates ((d)) based on the average of the differences in the rates calculated from the change over hrs 0–6 in the forecasts in the given test

period. (a) Control $\partial\theta/\partial t_{LW}$. (b) Experiment $\partial\theta/\partial t_{LW}$. (c) Experiment–Control $\partial\theta/\partial t_{LW}$. (d) Experiment–Control $\partial\theta/\partial t_{Total}$.

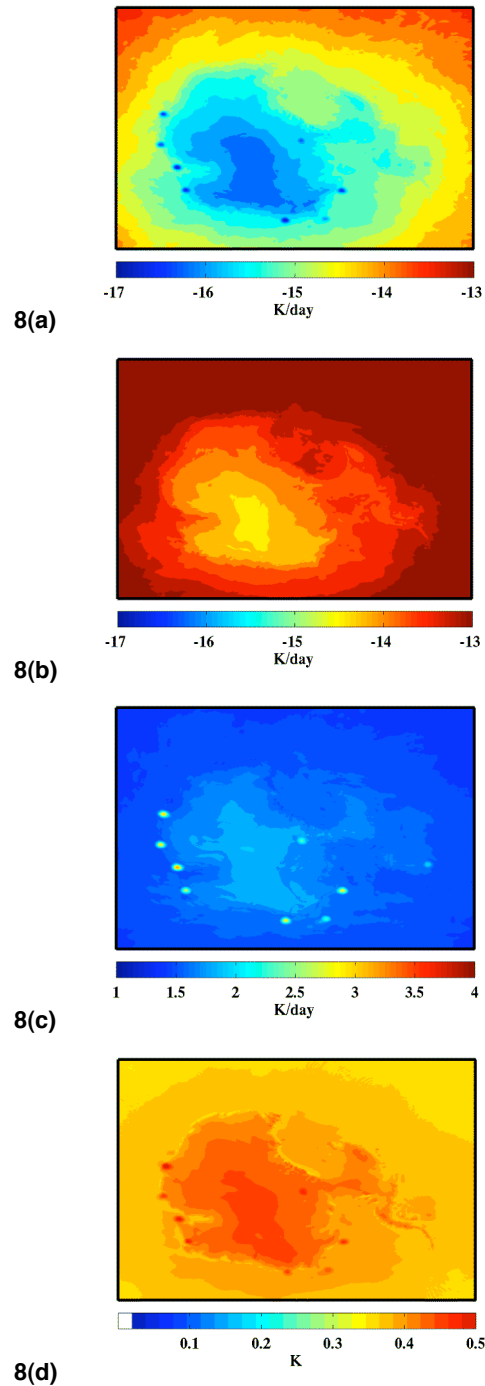


Fig. 8: Heating rates from LW and total in AMPS WRF tests for summer (January 2010) period. $\partial\theta/\partial t$ LW rates ((a), (b), (c)) based on instantaneous values for forecasts at hr 6. Total $\partial\theta/\partial t$ rates ((d)) based on the average of the differences in the rates calculated from

the change over hrs 0–6 in the forecasts in the given test period. (a) Control $\partial\theta/\partial t_{\text{LW}}$. (b) Experiment $\partial\theta/\partial t_{\text{LW}}$. (c) Experiment–Control $\partial\theta/\partial t_{\text{LW}}$. (d) Experiment–Control $\partial\theta/\partial t_{\text{Total}}$.

5. SUMMARY AND CONCLUSIONS

Previous investigations by one of the authors had uncovered biases in WRF radiative heating rates near the model's top, leading to excessive cooling at upper levels. The problem stems from the RRTM longwave scheme's approach to calculating radiative processes at the model top and of assumptions of the temperature and moisture applied in the stratosphere. This problem is being investigated in the context of the Antarctic Mesoscale Prediction System (AMPS), a real-time implementation of WRF over Antarctica.

Experiments with a modified RRTM longwave package running in WRF in AMPS have been conducted. The RRTM modifications refine its computational buffer layer above the model top and implement more accurate profiles of temperature and moisture to the top of the atmosphere (TOA). The modifications reduce the excessive cooling in WRF for the given regions, with the impacts being greater in the summer. They also correct erroneous LW cooling that may result from biases in relative humidity values at high levels seen in some radiosonde data over Antarctica. The results indicate that the modified RRTM scheme will reduce upper-level temperature biases over the 5-day forecasts. Based on this study, the modified RRTM longwave package for WRF has been implemented in AMPS, and it is now running operationally.

REFERENCES

- Cavallo, S.M., J. Dudhia, and C.M. Snyder, 2010: An improved upper boundary condition for longwave radiative flux in the stratosphere to correct model biases. *Mon. Wea. Rev.* (submitted)
- Ellingson, R.G., J. Ellis, and S. Fels, 1991: the intercomparison of radiation codes used in climate models: Long-wave results. *J. Geophys. Res.*, **96** (D5), 8929–8953.
- Mlawer, E.J., S.J. Taubman, P.D. Brown, M.J. Iacono, and S.A. Clough, 1997: Radiative transfer for inhomogeneous atmospheres: RRTM, a validated correlated-k model for the longwave. *J. Geophys. Res.*, **102** (D14), 16663–16682.
- Powers, J.G., A.J. Monaghan, A.M. Cayette, D.H. Bromwich, Y.-H. Kuo, and K.W. Manning, 2003: Real-Time mesoscale modeling over Antarctica: The

Antarctic Mesoscale Prediction System (AMPS). *Bull. Amer. Meteor. Soc.*, **84** 1533–1546.

Skamarock, W.C., J.B. Klemp, J. Dudhia, D.O. Gill, D.M. Barker, M.G. Duda, X.-Y. Huang, W. Wang, and J.G. Powers, 2008: A description of the Advanced Research WRF Version 3. NCAR Tech. Note, NCAR/TN-475+STR, 113 pp.